Sulfate Attack on Sulfate-Resistant Portland Cement Containing Limestone Filler

Ataque de sulfatos sobre los cementos Pórtland altamente resistente a los sulfatos conteniendo filler calcáreo

E.F. IRASSAR [a]
V.L. BONAVETTI [b]
M.A. TREZZA [c]
G. MENÉNDEZ [d]

Abstract

Limestone filler is an extended supplementary material used in the formulation of European and Latin American cements. Also limestone filler is being used to produce self-consolidating concretes. In a sulfate environment, the presence of limestone filler in cement increases the deterioration risk and can lead to the formation of thaumasite.

This paper presents results of expansion test conducted in accordance with ASTM C 1012 and the microstructural analysis on cement pastes with sulfate-resistant portland cement (SRPC) (C_3A < 2%) containing 12 and 18 % of limestone filler. Specimens were exposed to sulfate solution for three years at 20°C and 5°C. The evolution of attack was determined using XRD analysis on the material obtained from near surface layers of the specimens. Complementary, IR studies were carried out. Results show that SRPC containing 18 % limestone filler was more susceptible to sulfate attack than SRPC and SRPC with 12 % of limestone filler. The attack was characterized by the inward front leading first to the formation of ettringite, later formation of gypsum and finally thaumasite formation. All specimens present greater deterioration at low temperature.

Keywords: Limestone filler; Sulfate attack; Sulfate resistant portland cement; Thaumasite; XRD-analysis.

Resumen

El filler calcáreo es un material suplementario con un amplio uso en la elaboración de cementos en Europa y Latinoamérica. Este material también se ha comenzando a utilizar en los hormigones autocampactantes. En ambientes con sulfatos, la presencia de filler calcáreo en el cemento puede incrementar el riesgo de deterioro y conducir a la formación de thaumasita.

En este trabajo se presentan los resultados del ensayo de expansión realizado de acuerdo a la norma ASTM C 1012, y el análisis de la microestructura de prismas de pasta elaborados con un cementos portland resistente a los sulfatos (SRPC) (C_3A < 2%) conteniendo 12 y 18 % de filler calcáreo. Las probetas fueron expuestas en una solución de sulfatos durante 3 años a una temperatura de 5 y 20 °C. La evolución del ataque fue determinada sobre el material de la capa superficial de las probetas utilizando el análisis por DRX. Complementariamente, se realizaron estudios utilizando espectroscopia IR. Los resultados obtenidos muestran que el cemento SRPC conteniendo 18 % de filler calcáreo fue más susceptible al ataque de sulfatos que el cemento SRPC sin adición y el cemento conteniendo 12 % de filler calcáreo. El ataque es caracterizado por un frente de penetración que conduce primero a la formación de ettringita, luego la formación de yeso y finalmente la formación de thaumasita. Todas las probetas presentaron un mayor grado de deterioro a baja temperatura.

[a] ACI member E.F. Irassar is professor in the Department of Civil Engineering at the University of Center of Buenos Aires State, Olavarría, Argentina. He is Specialist on Concrete Technology of University of La Plata and head of INMAT Research Group. His research interests include blended cements, sulfate attack and durability.

[b] V. L. Bonavetti is professor in the Department of Civil Engineering at the University of Center of Buenos Aires State. She has received MSc in Concrete Technology. Her current research interest is concretes with limestone blended cements.

[c] M.A. Trezza is professor in the Department of Chemical Engineering at the University of Center of Buenos Aires State. She has received MSc in Concrete Technology. Her current research interest is waste fuel in portland cements and its chemical degradation.

[d] G. Menéndez is lecture in the Department of Civil Engineering at the University of Center of Buenos Aires State. He is MSc. candidate in Concrete Technology and his research interest is ternary blended cements.

1   Introduction

Since 1990, the increase of limestone filler addition during the manufacture of cement has contributed to increase the interest in studying thaumasite formation in concretes exposed to sulfate environments. In this case, the limestone filler is the internal source that provides the carbonate ions needed for thaumasite formation. The rate of this reaction is greatly increased at cold temperature below 15 °C and this type of sulfate attack may progress in concretes made with sulfate-resistant portland cement (SRPC) (1).

South-American regions have a mild climate, the mean temperature is in the range of 15 – 30 °C, and the production of portland limestone cement (PLC) containing up to 20 % of limestone filler has growth during the last years. For this reason, it is important to determine the sulfate performance of PLC, especially in the blended cements made with sulfate-resistant portland clinker at different temperature. The risk of sulfate attack increases in concrete foundation structures because the presence of sulfate ground waters at temperature below 15 °C is likely to occur.

A review on the sulfate attack on PLC show that most of laboratory experiments were carried out using portland clinkers with high or moderate C_3A content. Hooton (2) has studied a low level of cement replacement by limestone filler (5%) in cement with high or moderate C_3A content. Hartshorn et al. (3,4) report a worse performance of paste and mortar containing a Portland cement with moderate C_3A and 35 % of limestone filler exposed to cold (5°C) solution. Barker and Hobbs (5) studied the performance of Portland cement with high C_3A and PC with 15 % of limestone filler exposed to cold (5 °C) $MgSO_4$ solution (0.42 %) and Na_2SO_4 sulfate (0.42 %) and the prisms with limestone showed a more extended surface damage. Tsivilis et al. (6) also used an ordinary Portland clinker to make PLC and to prove the effect of a second active mineral addition on its sulfate resistance. Justnes (7) using a Norwegian standard cement with 20 % of limestone filler, the mortar expanded rapidly after 10 months of exposure in Na_2SO_4 at 5°C, indicating its worse performance.

However, studies using SRPC show different trends on sulfate performance. Our studies (8, 9) reveal that limestone filler addition decreases the sulfate resistance of moderate and low C_3A portland cement. On the other hand, Italian researchers (10) report that the damage of pastes and mortars of portland cements containing limestone filler exposed to cold (5 °C) $MgSO_4$ solution could be mitigated using a sulfate-resistant portland clinker.

The objectives of the present paper were to compare the performance and the mechanism of sulfate attack on the sulfate resistant cement with limestone filler exposed to different external sulfate solutions at different temperatures.

2   Experimental

This experimental investigation was carried out using a sulfate resistant portland cement (C0F), similar to ASTM Type V, and two limestone portland cements (C12F and C18F) obtained from the same portland clinker by an intergrinding process in the cement plant. The potential composition of portland clinker was C_3S = 58 %, C_2S = 18 %, C_3A = 2 % and C_4AF = 13 %, and the limestone content by mass was 0, 12 and 18 % according the data supplied by the cement producer. Cements have the same strength class (CP40, f´$_c$ > 40 MPa at 28 days tested on ISO-RILEM prisms) leading to a large specific surface of limestone blended (321, 380 and 383 m²/kg for C0F, C12F and C18F cement, respectively). The chemical composition and physical characteristics of cements used are given in Table 1. Low C_3A content of all used cements was checked by XRD analysis.

Table 1: Chemical composition and Physical characteristics of cementing materials used

	Cement		
	C0F	C12F	C18F
Chemical composition, %			
SiO_2	21.44	19.96	19.75
Al_2O_3	3.40	3.28	3.14
Fe_2O_3	4.20	3.91	3.35
CaO	63.45	61.77	61.42
MgO	0.57	0.56	0.57
K_2O	1.18	1.01	0.92
Na_2O	0.04	0.02	0.04
SO_3	2.91	2.77	2.75
Loss by ignition	1.82	5.86	7.25
Physical characteristics			
Specific gravity	3.15	3.09	3.06
Specific surface (Blaine), m²/kg	321	380	383
Retained on sieve, %			
75 µm (#200)	3.9	3.8	9.7
45 µm (#325)	16.4	14.5	25.7
Position parameter $x*$, µm	28.81	22.66	31.13
Homogeneity parameter, n **	0.93	0.95	0.86

* Characteristic diameter of particle size distribution obtained at cumulative mass of 63.2 %

** Slope of particle size distribution curve representing the wide of distribution

2.1   Mortar Specimens

For each cement, a series of mortar specimens (285 x 25 x 25 mm³) was cast according to ASTM C 1012 (sand-to-cementitious material ratio of 2.75 and w/cm of 0.485). Mortar specimens were stored in moist cabinet during 24 hours, and then they were removed from the mold and cured in saturated lime-water solution until 28 days. After curing, each series of prisms was individually immersed (volume of sulfate-solution to mortar-bars = 4:1) in plastic tank containing a 5% Na_2SO_4 solution (0.352 M) at room temperature (20 ± 2°C). The pH of test solution was checked using a few drops of phenolphthalein as pH-indicator and the solution was renewed as necessary.

For blended cement with high sulfate-resistant cement, the expansion limits are 0.05 % and 0.10 % at 6 and 12

months, respectively according to ASTM C 1157. At three years, the external layer of specimens was analyzed by X-ray diffraction by to determine its mineralogical composition.

2.2 Paste Specimens

Prisms (25 x 25 x 40 mm^3) were cast using a cement paste with water w/cm of 0.5. For this w/cm, the paste was mixed in a high speed domestic blender, and carefully remixed to avoid bleeding. After 24 hours in moist cabinet, paste prisms were demolded, transferred to plastic tank and water cured for further 27 days at 20 °C. After this initial period of hydration, surfaces of the specimens were epoxy-coated with the exception of one surface perpendicular to molding and then immersed in water during 24 hours for saturation of specimens. Then, paste prisms were divided in two groups and totally immersed in plastic recipient containing a combined sulfate solution (0.176M Na_2SO_4 and 0.176 M $MgSO_4$) with a few drop of pH indicator. One group was stored at room temperature (20°C) and the others were stored at 5 °C.

After 90, 180, 365, 720 and 1080 days, all prisms were visually examined and the surface change were registered. A selected prism was used to determine the compound formed during sulfate attack at different depths using X-ray diffraction (XRD) and Fourier transformed infrared spectroscopy (FTIR). At a given age, prisms were immersed in acetone and then dried at 40 °C overnight. Subsequently, using the wearing device, layers of 1 mm depth were obtained from the surface to the core of the specimen. The powdered material was obtained by cutting perpendicularly to the prism face at 5 mm from both edges of the prism. The material form each layer was collected and ground to pass through 45 µm sieve (#325) and stored in a sealed plastic bag to prevent carbonation before XRD and FTIR analysis.

XRD measurements were performed on Philips X'Pert diffractometer equipped with a graphite monochromator using CuKα radiation and operating at 40 kV and 20 mA. Step scanning was used with a scan speed of 2°/min and sampling interval of 0.02° 2θ. FTIR spectra were recorded using a NICOLET Model Magna 500. The pellets were prepared using potassium bromure (KBr) technique and the spectrum was recorded in the range 4000 – 400 cm^{-1}.

3 Results and discussion

3.1 Mortar Specimens

Fig. 1 shows the visual appearance of mortars bars after 3 years. In all cases, the first sign of attack was the deterioration of the corners followed by cracking along the edges. For C18F mortar, this sign was manifested after 180 days and subsequently, specimens expanded rapidly and finally, they exhibited a large curvature and large cracks. However, specimens did not present an extensive surface softening and they remained still solid. In contrast, the C0F and C12F mortars required more than two years in sulfate solution to show the first visual sign of deterioration. At three years, they presented some fine cracking along their edges but their core was still intact.
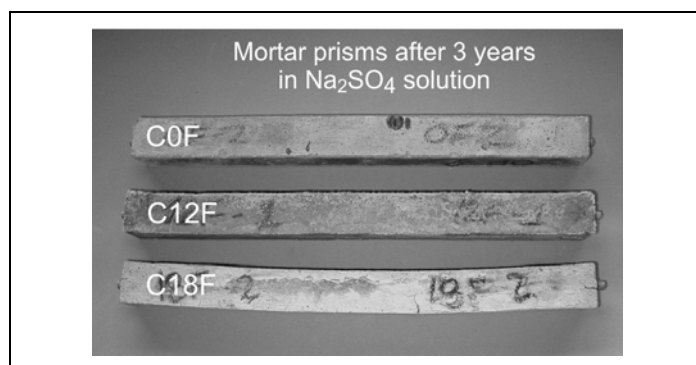

Figure 1 - Visual appearance of ASTM C 1012 mortars prisms exposed by 3 years to Na_2SO_4 solution.

Data on expansion of mortar prisms in sulfate solution are shown in Fig. 2. These data indicate that C12F mortar has the lowest expansion during the test, while C18F mortar has a higher expansion during duration of test, instead of the low C_3A^- content in this cement.

At 6 months, all cements had expansion lower than 0.05 % and could be considered as "high sulfate-resistant". Subsequently, C18F cement has failed to qualify as "sulfate resistant-cement" because it had an expansion of 0.148 % at 365 days. In contrast, expansion of C12F cement was lower (0.040% at 365 days) than the failure limits proposed for sulfate resistant cement (0.050 at 180 days and 0.10 % at 365 days). Similar trend was observed in mortar bars made with C0F cement. After one year, it should be noted that C12F continued to expand at only a low rate. However, there was an increase of expansion rate in C0F mortar beyond one year.
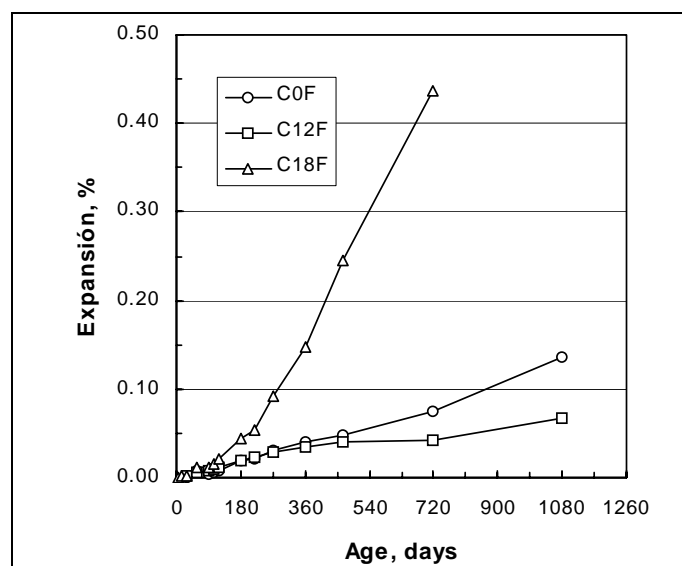

Figure 2 - Expansion of mortar prisms in Na_2SO_4 solution.

Fig. 3 shows the mass variation of these specimens. It was observed that there was a little gain of mass in mortar bars of all cements during all exposure time. It is interesting to see that the mass gain is associated with the expansion during all exposure time. Specimens with C18F cement have a higher mass increase and expansion. Also the mass gain indicates that there were not spalled pieces of prisms.
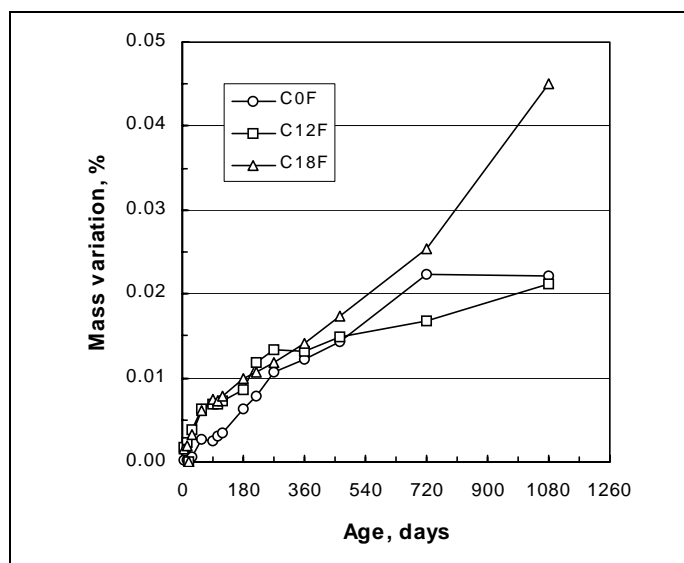
Figure 3 - Mass variation of mortar prisms in Na_2SO_4 solution.

XRD patterns of surface layer of mortar prisms are shown in Fig. 4. Diffractgrams show that gypsum ($2\theta = 11.60°$) is the main product of sulfate attack for all mortars exposed to Na_2SO_4 solution. Also, mortars present the complete depletion of CH and its peaks at 2θ 18.09° is absent. C0F mortar exhibits a calcite peaks ($2\theta = 29.41°$, 23.02°). In mortars containing C12F cement, gypsum peaks appear accompanied by some ettringite peaks ($2\theta = 9.09°$, 15.8°). There was no evidence of the presence of thaumasite peaks ($2\theta = 9.15°$, 16.0°) in both mortars with PCL.
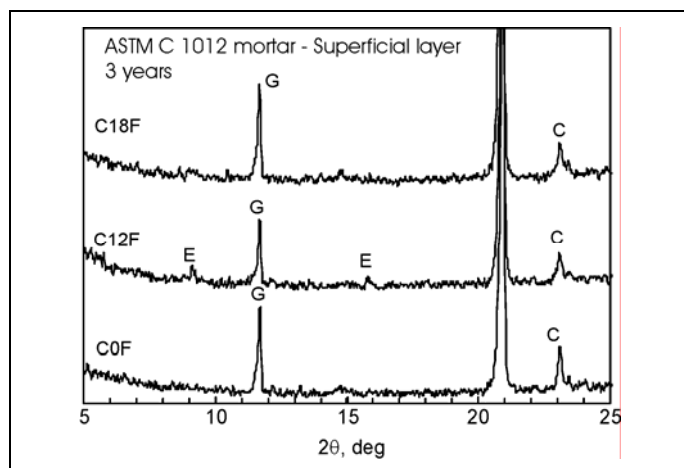

Figure 4 - XRD patterns of superficial sample of the mortar prisms after 3 years in Na_2SO_4 solution. (E = ettringite, G = gypsum, C = calcite).

It should be noted that the effective w/c of mortars made with C18F (0.59) is higher than the C0F (0.485), and the potentially higher permeability may have resulted in deeper penetration of sulfate ions.

3.2 Paste Specimens

Photograph of specimens stored in combined sulfate solution for three years are presented in Fig. 5. All prisms of C0F, C12F and C18F stored at 20 °C show no visible

damage signs after three years. However, prisms stored at 5°C shown a progressive deterioration. A severe damage was observed at the corners and edges of the prisms and its surface layer was peeling and had spalled causing some mass loss after three years. The C18F prisms present the worse visual appearance. The progress of visual appearance of paste is quite similar to the process described by Tsivilis et al (6).
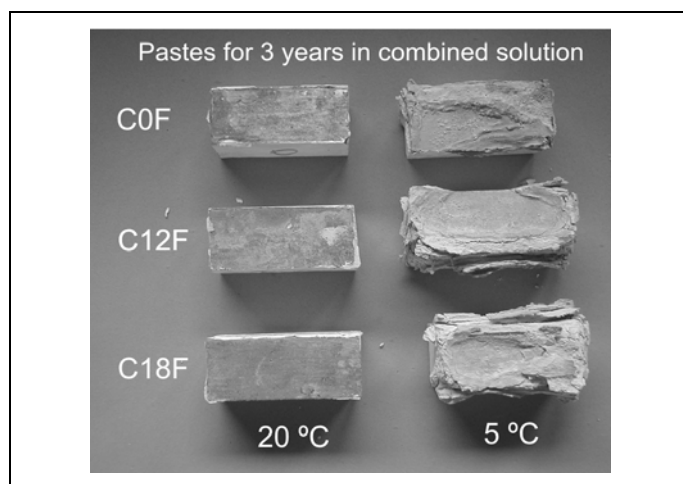

Figure 5 - Visual appearance of paste prisms exposed by 3 years to combined solution at 5 and 20 °C.

The XRD analysis of the surface layer of prism stored at 20°C is shown in Fig. 6. Diffractograms reveal the formation of ettringite in these layers, the presence of CH and they also show that gypsum is absent for all cement used. There was a surface carbonation of specimens and XRD reveals the presence of calcium carbonate crystals in calcite and aragonite forms. It is known that aragonite precipitates in presence of magnesium ions. At the exposed surface, thaumasite was not detected at this temperature.
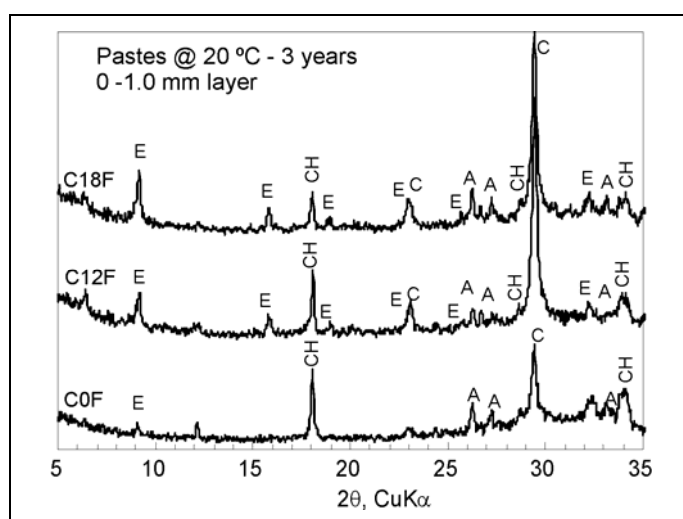

Figure 6 - XRD patterns of superficial material of paste prisms after 3 years in combined sulfate solution at 20 °C. (E = ettringite, CH = calcium hydroxide, C = calcite, A = aragonite).

According to superficial analysis, C18F cement prisms appear to be the more susceptible to attack because a large amount of ettringite and small amount of CH were found.

When simples from various depths were analyzed (Fig. 7), it was observed that the intensity of CH peaks ($2\theta = 18.09°$ and $2\theta = 34.09°$) increase significantly in the deeper layers, while the main ettringite peak ($2\theta = 9.08$) decrease. For low C_3A cements, ettringite formation may be the result of the reaction between sulfate ions and the ferroaluminate hydrates (9). It is noted that for the layer at 3.5-4.5 mm depth, the main peak of calcium monocarboaluminate (AFm phase in PLC) is detected at $11.67°$ 2θ. It was also determined that small peak of quartz ($2\theta = 26.64°$) is due to impurities present in limestone used.
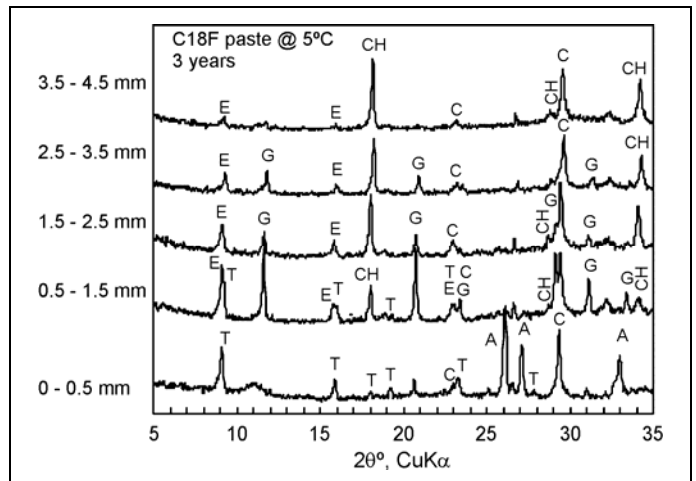
The layer by layer XRD-analysis of prisms stored at 5°C for C0F, C12F and C18F cements are shown in Figs. 8, 9 and 10, respectively. For all cements, it is observed that the depth of sulfate attack is limited to few millimeters from the surface and the material spalled on the surface of prism is quite different containing mainly thaumasite, ettringite, gypsum and aragonite.
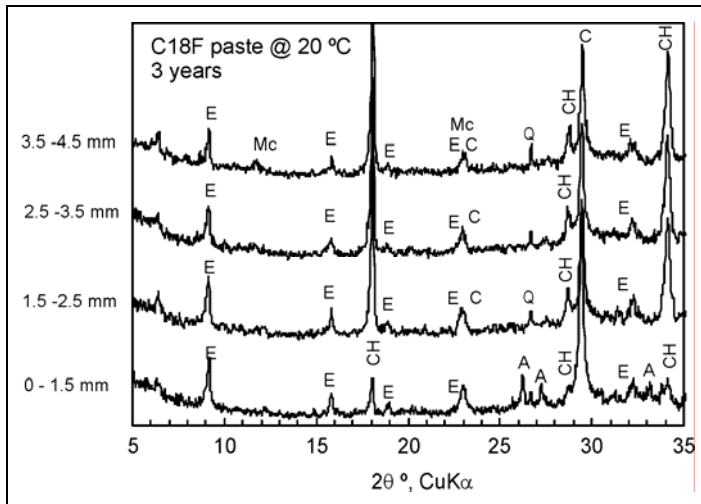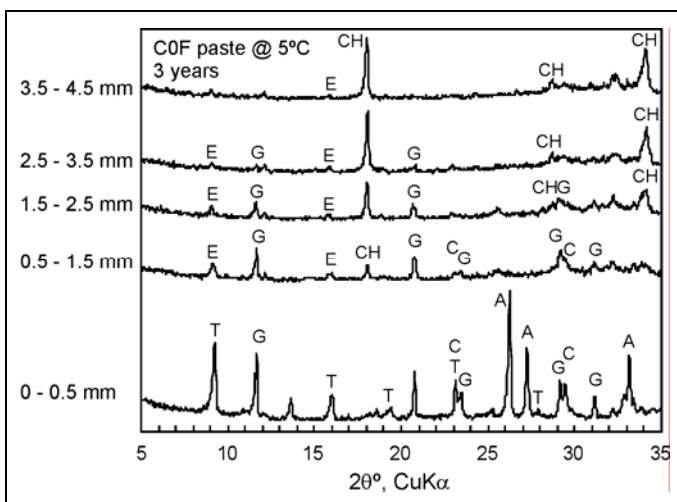

Figure 7 - Layer by layer XRD analysis of C18F paste stored at 20 °C in combined sulfate solution.
(E = ettringite, Mc = calcium monocarboluminate, CH = calcium hydroxide, C = calcite, A = aragonite).

Figure 8 - Layer by layer XRD analysis of C0F paste stored at 5 °C in combined sulfate solution.
(T = thaumasite, G = gypsum; E = ettringite, CH = calcium hydroxide, C = calcite, A = aragonite).
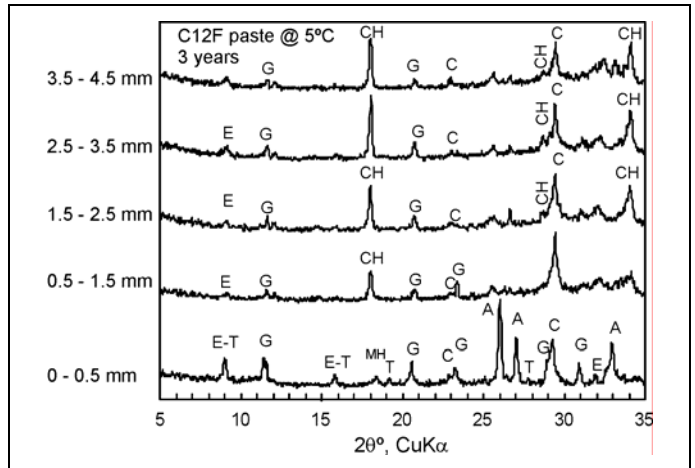
Figure 9 - Layer by layer XRD analysis of C12F paste stored at 5°C in combined sulfate solution.
(T = thaumasite; E = ettringite, CH = calcium hydroxide, MH = magnesium hydroxide;C = calcite, A = aragonite).

Figure 10 - Layer by layer XRD analysis of C18F paste stored at 5 °C in combined sulfate solution.
(T = thaumasite, E = ettringite, CH = calcium ydroxide, C = calcite, A = aragonite).

For C0F cement, the main crystalline compounds found on the spalled layer due to degradation process were thaumasite, gypsum and aragonite (Fig. 8). Also, there was little proportion of CH and calcium carbonate crystallized in calcite form. In this material, the thaumasite was identified by its characteristic peak at $2\theta = 19.35°$. In the 0.5-2.5 mm and 2.5-3.5mm layers, the intensity of CH peaks increases and both ettringite and gypsum compounds were found. Finally, characteristic sulfate attack compounds are absent at the 3.5-4.5mm layer.

Fig. 9 shows the XRD patterns of layers for C12F cement after 3 years. It is observed that a this paste exhibit a little variation from the 0.5-1.5 mm to 3.5-4.5 mm layer. The spalled material is also characterized by the formation of ettringite-thaumasite and gypsum due to the sulfate attack and aragonite due to the carbonation. XRD – pattern also showed a small amount of brucite (MH) detected by its peak at 18.5° 2θ.

For C18F paste (Fig. 10), XRD-analysis shows a severe alteration of the spalled layer. Thaumasite is clearly identified and it is accompanied by aragonite. At 0.5-1.5 mm layer, ettringite and thaumasite coexist according to XRD analysis. It is very clear the doublet peaks at 15.8°, 18.93° and 23.0° 2θ and the deformation of the main peak of ettriginte-thaumasite (9.09° and 9.15° 2θ). Also, some small peaks can be used to identify the presence of either ettringite or thaumasite. In particular, the thaumasite peak at 19.35° 2θ is absent in the ettringite pattern. Likewise there is an ettringite peak that has no equivalent in the thaumasite pattern at 22.96° 2θ but it is very close to the $CaCO_3$ peak corresponding to the limestone filler. There was also large proportion of gypsum in this layer. The sulfate attack compounds decreases from the surface to the deeper layers. At 3.5-4.5 mm depth, there was an unattacked layer showing ettringite and a poorly crystallized AFm phase centered upon the main monocarboaluminate peak.

As in XRD pattern, the spalled material presents a FTIR spectrum (Fig. 11) quite different than those samples obtained from the first millimeter of paste. In this sample, the characteristic mode of calcium carbonate in aragonite form can be identified. Aragonite is clearly recognized by: ν3 mode in 1500cm^{-1}, ν2 splitting in 845 (w) and 855 cm-1(s) as well ν4 in 702(w) and 715(m) cm^{-1}; ν1 active in 1083 cm^{-1} and associated bands in 1785 cm^{-1}. The SO_4^{2-}-group is revealed through the peak in 1100 cm^{-1} zone, however gypsum or ettringite can not be completed assigned. Nevertheless, this group can be associated to different compounds which present the SO_4^{2-} group. Additionally, identified bands were: water deformation in 1600 cm^{-1} zone, asymmetrical stretching ν3, SiO_4 centered in 925 cm^{-1} and bands associated to free OH groups in the high zone. FTIR spectra of samples taken at different depth are very similar and Fig. 11 shows 2.5-3.5 mm layer. In the high zone, two characteristic peaks were identified, 3645cm^{-1}, associated to groups OH$^-$ of the CH formed during the hydration and one in 3400 cm^{-1}, ν3 water associated to ettringite. At 1600cm^{-1}, it was found the peak assigned to free water, ν2. The pronounced peak centered in 1400cm^{-1} is assigned with this located in 875 and 713cm^{-1} to the carbonate group, in its calcite form, present in C18F cement. The remaining peaks correspond to the sulfate group; the asymmetric stretching of this group generates a characteristic band around 1100cm^{-1}. The doublet to 1120 and 1145 cm^{-1} present in gypsum is transformed into an only one peak (in 1118cm^{-1}), when ettringite is present (12). In the low zone, it was ν2 and ν4 SO_4^{2-} in 420 and 670 cm^{-1}, respectively associated to ettringite. The peak to 859 cm^{-1} can be assigned to the Al-O-H stretching and also attributed to the ettringite presence (13)

4   Summary

The results of this investigation indicates that the damage produced by sulfate solutions increase as the level of limestone filler replacement increased in PLC, formulated with low C_3A clinker. In Na_2SO_4 solution, the expansion increases for C18F cement and the alteration zone of cement paste exposed to combined solution at 5°C was deep. In the authors' opinion, based on previously

experimental evidences (14), when large replacements of filler are used in the PLC formulation, there is an increase of permeability of well cured mortar or concrete. It is due to the increase of the effective w/c in the mixtures because limestone filler does not produce a pore size reduction.
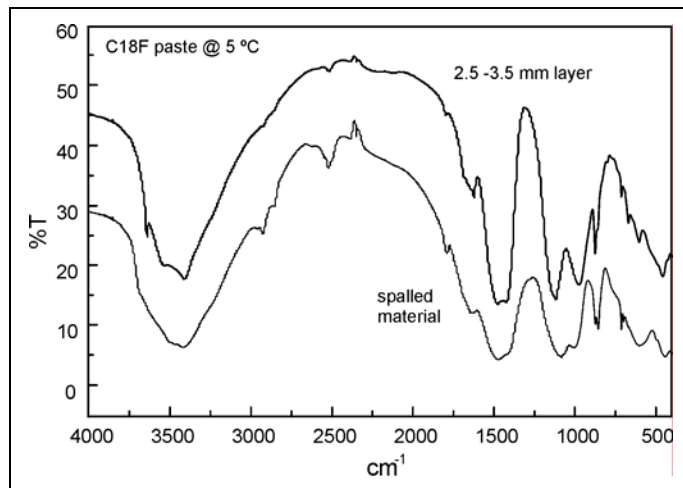
Figure 11 - FTIR spectra of spalled material and 2.5 – 3.5 mm layer of C18F paste stored at 5 °C in combined sulfate solution.

According to previous XRD studies on moderate C_3A cement (14) and the studies presented here, the sulfate attack is a progressive phenomenon from the surface inwards and involves several stages. The sequence of attack includes the following stages:

1) Diffusion of SO_4^{2-} into the matrix and CH leaching which is governed by the matrix permeability.

2) Ettringite formation governed by the presence of AFm phases in the paste (monosulfoaluminate, monocarboaluminates or hydrates from C_4AF), and its expansiveness governed by the presence of saturated calcium solution.

3) Gypsum formation and depletion of CH, when the ettringite expansion causes the disruption of paste structure and the sulfate ions ingresses easily and reacts with CH to form gypsum.

4) Decalcification of C-S-H, the severe depletion of CH produced by sulfate or magnesium attack cause the instability of CSH and its breakdown. This process is more severe in solutions containing magnesium sulfate.

5) Thaumasite formation as results of the reaction of ettringite previously formed and the silica provided by the breakdown of CSH.

At low temperature, the attack is more severe on the surface layers for all cements (including the SRPC without limestone). The authors suggest that ettringite is more expansive in this condition due to the large solubility of calcium and improving the stability of ettringite. On the other hand, authors believe that the protective layer caused by brucite and carbonates is spalled by the large expansiveness of ettringite formed below the surface. Then, thaumasite is the main attack product of the disrupted layers.

5 References

[1] N. J. Crammond, M. A. Halliwell, "The thaumasite form of sulfate attack in concretes containing a source of carbonate ions - a microstructural overview", in: Second CANMET/ACI International Symposium on Advances in Concrete Technology, SP-154, American Concrete Institute, USA, 1995, 357-380.

[2] R.D. Hooton, "Effects of carbonate additions on heat of hydration and sulfate resistance of portland cements", in: P. Klieger, R.D. Hooton (Eds.), Carbonate Additions to Cement, ASTM STP 1064, 1990, 73-81.

[3] S.A. Hartshorn, J.H. Sharp, R.N. Swamy, "Thaumasite formation in Portland-limestone cement pastes". Cement Concrete Research 29, 1999, 1331-40,

[4] S.A. Hartshorn, J.H. Sharp, R.N. Swamy. "The thaumasite form of sulfate attack in Portland-limestone cement mortars stored in magnesium sulfate solution". Cement Concrete Composites 24, 2002, 351-599;

[5] A.P. Barker, D.W. Hobbs, "Performance of Portland limestone cements in mortar prisms immersed in sulfate solutions at 5 °C", Cement Concrete Composites 21 (2) 1999, 129-137.

[6] S. Tsivilis, A. Kakali, A. Skaropoulou, J.H. Sharp, R.N. Swamy. "Use of mineral admixtures to prevent thaumasite formation in limestone cement mortar". Cement Concrete Composites 25 (8) 2003, 969-976.

[7] Harald Justnes. "Thaumasite formed by sulfate attack on mortar with limestone filler", Cement Concrete Composites 25, (8) 2003, 955-959.

[8] E.F. Irassar, M. González, V. Rahhal, "Sulphate resistance of Type V cements with limestone filler and natural pozzolan", Cement Concrete Composites 22 (5) 2000, 361-368.

[9] M.A González, E.F. Irassar, "Effect of limestone filler on the sulfate resistance of low C3A Portland cement", Cement Concrete Research 28 (11) 1998, 1655-1667.

[10] A. Brosoi, S. Collepardi, L. Copolla, R. Troli, M. Collepardi, "Sulfate attack on blended portland cement", in: V.M. Malhotra (Ed),. Proc. Fifth CANMET/ACI International Conference on Durability of Concrete, Barcelona, Spain, ACI SP 192, 2000, I, 417-432.

[11] M.A. González, E.F. Irassar, "Ettringite formation in low C3A portland cement exposed to sodium sulfate solution", Cement Concrete Research 27 (7) 1997, 1061-1072.

[12] J Bensted, "Characterisation of sulphate wavebands in the infrared spectra of cement minerals", Il Cemento 87 (3) 1990, 137–146.

[13] S.M. Torres, J.H. Sharp, R.N. Swamy, C.J. Lynsdale, S.A. Huntley. "Long term durability of portland limestone cement mortars exposed to magnesium sulfate attack", Cement Concrete Composites 25, (8) 2003, 947-954.

[14] E.F. Irassar, V.L. Bonavetti, M. González. "Microstructural study of sulfate attack on ordinary and limestone portland cements at ambient temperature", Cement and Concrete Research, 33 (1) 2003, 31-41.